Disclaimer

This note has not been internally reviewed by the DØ Collaboration. Results or plots contained in this note were only intended for internal documentation by the authors of the note and they are not approved as scientific results by either the authors or the DØ Collaboration. All approved scientific results of the DØ Collaboration have been published as internally reviewed Conference Notes or in peer reviewed journals.

Latest results in fiber tracking from the DØ Upgrade*

R. C. Ruchti

Department of Physics, University of Notre Dame, Notre Dame, Indiana 46556, USA

for the

DØ Fiber Tracking Group

The DØ collaboration is upgrading its existing detector to provide enhanced functionality for physics in the Fermilab Main Injector Era, when the luminosity of the Tevatron Collider will evolve to levels in excess of 10^{32} cm^{-2} sec^{-1} in combination with reduction of the beam crossing interval to 132 nsec. The DØ upgrade retains the strengths of the existing detector which include hermetic coverage in fine-grained liquid argon calorimetry and muon detection using magnetized iron toroids and combines these with a new magnetic central tracking system based upon scintillating fiber and silicon strip technologies in a 2 Tesla solenoidal field. This paper summarizes briefly the elements of the upgrade and the central fiber tracker and presents recent measurements of performance of fiber tracking technology using the cosmic ray test facility at Fermilab.

INTRODUCTION

The DØ detector is designed to study high p_T physics at the Tevatron collider. This objective demands excellent sensitivity and efficiency for the detection of electrons, muons, photons, jets, and missing transverse energy. The key features of the design include fine-grained hermetic electromagnetic and hadronic calorimetry, hermetic muon detection with iron toroid magnets, and non-magnetic central tracking [1]. To date, this experimental platform has been highly successful in the study of physics of high p_T phenomena, culminating with the co-discovery of the top quark at Fermilab earlier this year [2].

Currently signals for signature high p_T physics processes are in the tens of thousands of events for W bosons into lepton channels and tens of reconstructed events for top quarks. To substantially extend the physics reach of the current collider experiments will require an order of magnitude increase in the luminosity of Tevatron Collider, which should be achieved when the Main Injector operation commences at the end of the decade. Luminosities of ~ 2 x 10^{32} cm^{-2} sec^{-1} are planned. To operate effectively at such luminosities is beyond the capability of the present experimental detectors, and hence new detectors and new detector technologies are required.

The strategy of the DØ Collaboration [3,4] is to build upon the present strengths of the DØ detector which include electromagnetic and hadronic calorimeter coverage to $|\eta| < 4.4$ and muon coverage to $|\eta| < 3$. A new magnetic central tracking system will provide the following: momentum measurement and charge determination; electron identification and first-level triggering; muon identification and first-level triggering (especially at low p_T); and tagging of b-quark decays by identification of displaced vertices. An elevation view of the upgraded detector is presented in Fig. 1.

DØ CENTRAL TRACKING

A key element of the upgraded DØ detector is the implementation of central tracking in a 2 Tesla solenoidal field [5]. Figure 2 displays the central tracking region which is instrumented with several new detector systems. Surrounding the collision region at radii less than 10 cm and covering $|\eta| < 3$ is a silicon vertex tracker (SVT) comprising seven barrel detector arrays, twelve small disk arrays, and four large disk arrays [6]. Each of the component array elements is a single-sided or double-sided detector of 300 μm thickness supporting strips with 50 μm pitch readout. Spatial resolution is of order 10 μm. The SVT system is assembled from 1344 individual detectors and contains 837K readout channels.

* Presented at SPIE'95, Optical Science, Engineering, and Instrumentation Symposium, July 10-14, 1995, San Diego, California.

providing 2 axial and 2 stereo measurements. Scintillating fibers are of 830 μm diameter and provide a spatial resolution per measurement of ~ 100 μm in the r-ϕ plane. The CFT system is comprised of 80K fibers read out with visible light photon counters (VLPC).

Placed just outside the coil of the superconducting magnet at a radius r ~ 70 cm is the central preshower detector (CPS) containing 6 K scintillation elements with waveshifting fiber and VLPC readout [7]. The CPS covers the central region $|\eta| < 1.3$. A forward preshower detector covers the intermediate and forward region ($1.4 < |\eta| < 2.5$) and is presently under design.

The central fiber tracker and the preshower detectors will be used for (and are fundamental to) first-level triggering for electrons, muons, and photons.

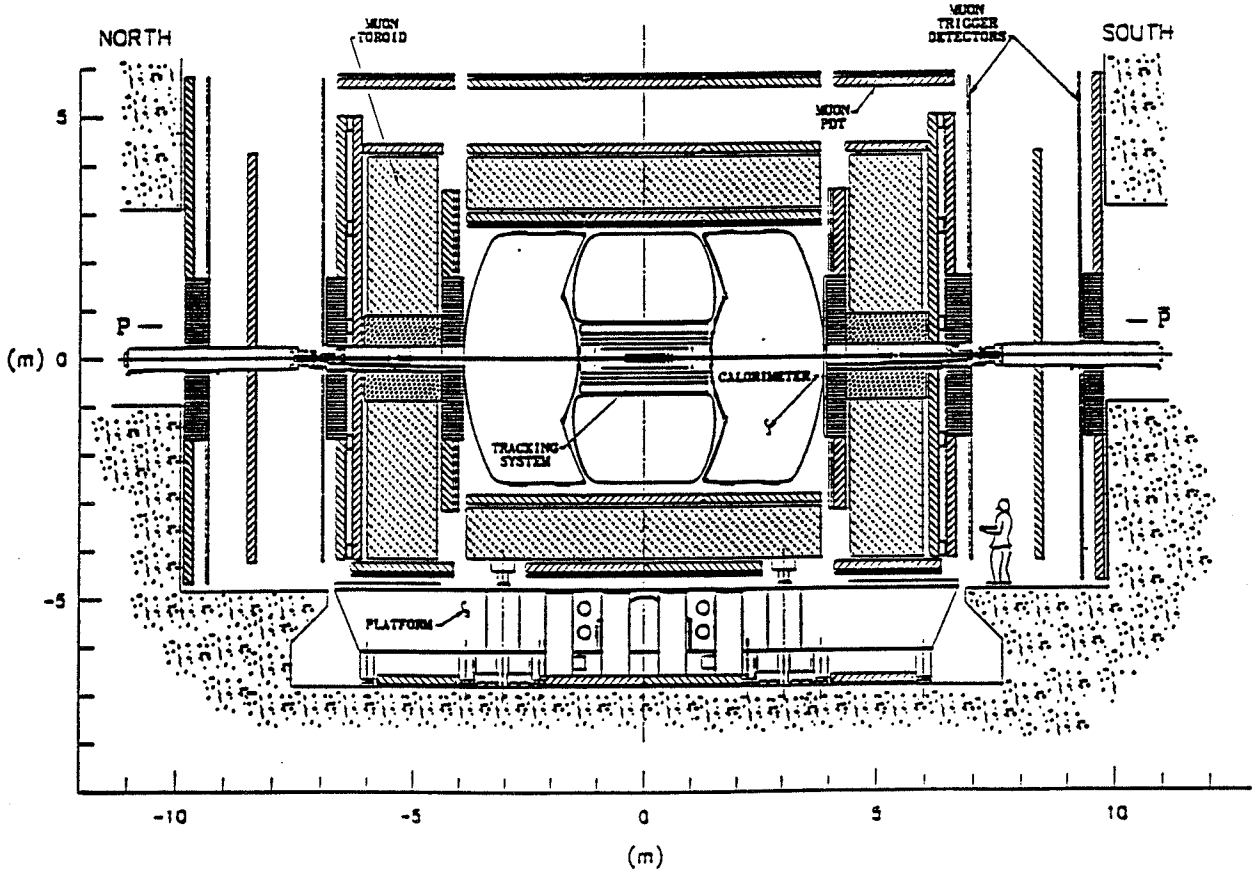

Figure 1. Elevation view of the DØ Upgrade Detector.

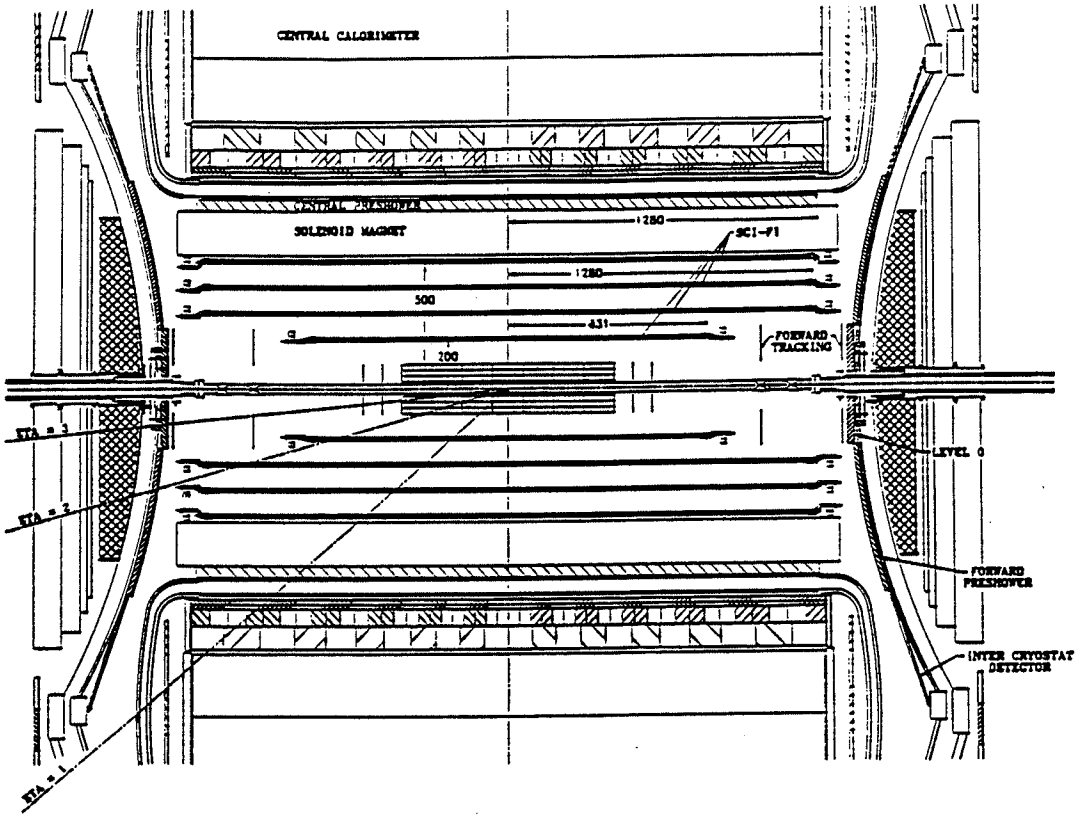

Figure 2. The central tracking system for the DØ Upgrade (dimensions in mm).

THE COSMIC RAY TEST FACILITY

Preparatory to construction of the fiber tracker, important system parameters under evaluation include: efficiency, operational stability, and capabilities for physics. We will discuss the first two topics here. Physics capability is addressed elsewhere [3,8].

Prototype detector elements for the DØ fiber tracker have been under continuous study for a period exceeding 1 year in a Cosmic Ray Test facility (CRT) located in Lab 6 at Fermilab. This facility, shown schematically in Fig. 3, is configured as follows: detector elements for study and test are placed atop a steel stack which is situated in a dark room; trigger counters are placed just above and below the detector elements and at two depths within the steel stack, corresponding to two minimum momentum thresholds p_{min} for cosmic ray muons which penetrate the stack. These thresholds are p_{min} = 0.8 GeV/c for muons which penetrate from above to the trigger layer midway through the steel; and p_{min} = 2.5 GeV/c for muons which reach the bottom. A four-fold (three-fold) cosmic ray trigger indicates the passage of a muon of at least 2.5 GeV/c (0.8 GeV/c) momentum through the fiber detector elements.

Additional tracking elements, Iarocci tubes, are also included to assist in tracking studies but play no role in triggering. These are also indicated in Fig. 3.

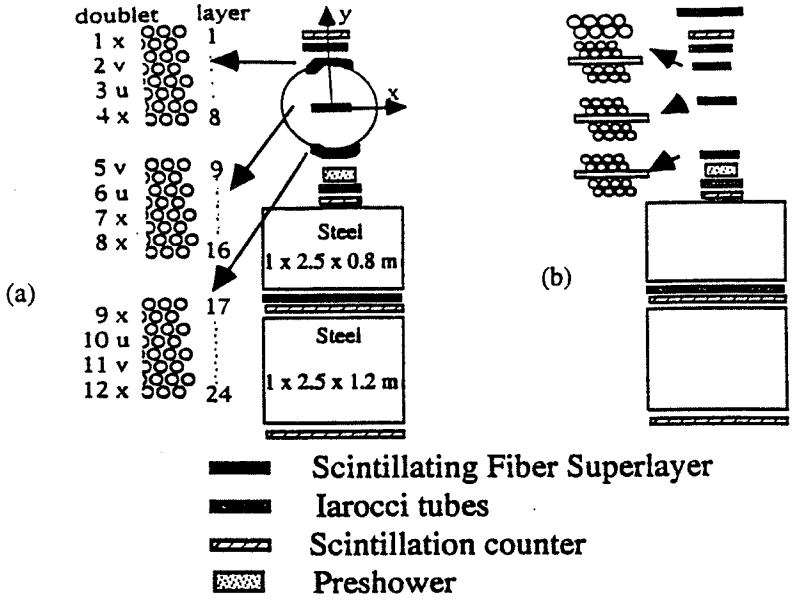

Figure 3. Schematic of the Cosmic Ray Test Facility: (a) initial configuration; (b) latest configuration.

The scintillating fiber doublet: The basic detection element of a fiber tracker is the scintillating fiber doublet, composed of two singlet fiber layers, with one layer offset by a halfspacing from the other as shown in Fig. 4. This assures that if an energetic particle traverses through the crack between fibers in one layer, it is likely to traverse the diameter of a fiber in the offset layer. Hence the fiber doublet efficiency is high, provided that the photoefficiency of the fiber materials is high.

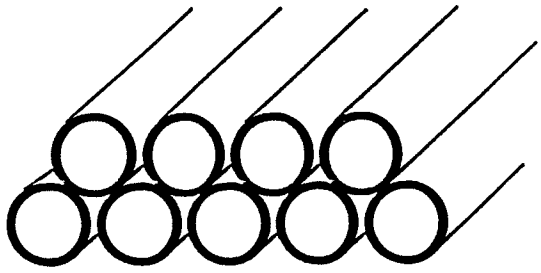

Figure 4. The fiber doublet, the basic detection and measurement element of a fiber tracker.

The fiber doublets are placed on cylindrical or planar mounting surfaces fabricated from low-mass composite materials as shown in Fig. 3. Superlayers are formed from several fiber doublets, including measurements of transverse coordinate (x, x′) as well as small angle stereo (u,v). For an 8 month period, the CRT was configured as in Fig. 3a, with three fiber superlayers composed of x,u,v, x′ fiber doublets. More recently, the CRT has been configured as in Fig. 3b, with three superlayers containing x and x′ doublet layers only. Here the x and x′ doublets offset by 1/4 fiber spacing.

Fiber structure and composition: A schematic of an single fiber detector element is shown in Fig. 5. It consists of a multiclad scintillating fiber of 830 μm diameter and 2.8 m length optically coupled to a multiclad waveguide fiber of 965 μm

diameter and 8 m length. The fibers are manufactured by Kuraray Corporation. The core material is polystyrene (n=1.59) , the inner clad is of PMMA (n=1.49), and the outer clad is a fluoro-acrylic (n=1.42). The polystyrene core of the scintillating fiber is doped with the fluorescent dyes p-terphenyl (1% by weight) and 3-hydroxyflavone (1500 ppm). Fluorescence emission maximum for this material is λ_{max} ~ 530 nm. Waveguide fibers are compositionally identical to the scintillating fibers except that they contain no fluorescent dyes. A foil mirror was placed at the far end of the scintillating fibers, to reflect scintillation light initially travelling in the direction away from the photosensor back into the fiber so that it can be detected.

Photosensor: The photosensor is the visible light photon counter or VLPC, a derivative of the solid state photomultiplier developed by Rockwell International Science Center [9]. The VLPC has been chosen because this device has a typical quantum efficiency > 60% for visible wavelengths, high gain (>15000), low gain dispersion (~15%), and an intrinsic time resolution of order 100 ps. The VLPC version used in these studies is the HISTE-IV VLPC and these are operated at cryogenic temperature, T ~ 6.5K.

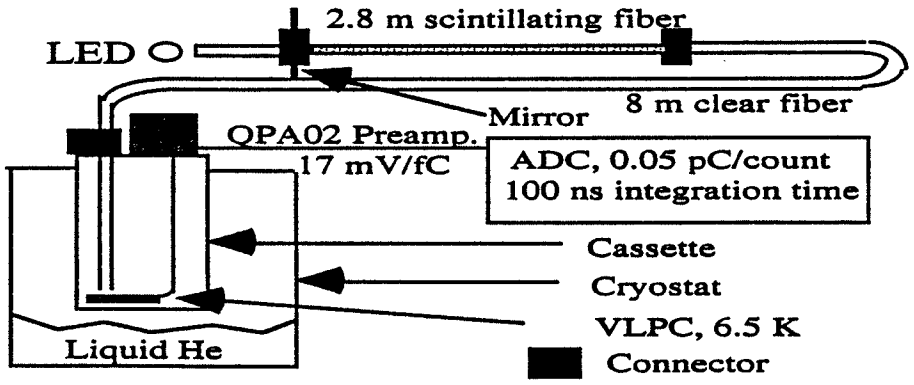

Figure 5. Schematic of a single fiber detector element.

System Performance

In previous papers, we have shown that a mean of ~ 10 photoelectrons is detected for scintillating fiber elements of the type described above, in bench tests of relatively small numbers of fiber channels [10]. This established proof-of-principle for fiber tracking technology. The goals of the present study are to assess system level performance, including long term stability of detector gain, gain dispersion, photoelectron yield, and mechanical robustness, and to study spatial resolution and cross talk.

Calibration of the Photoelectron Signal: The photoelectron yield for individual fiber channels is obtained by comparing the observed ADC spectrum of a given channel (Fig. 6a) for cosmic ray triggers, with the corresponding ADC calibration spectrum (Fig. 6b) obtained with that channel illuminated by a pulsed LED. In the CRT, each of the 3072 channels of the CRT has its own individually addressable calibration LED. As Fig. 6b indicates, the gain dispersion of the VLPCs is very low, allowing peaks corresponding to 0 (pedestal), and 1, 2, 3,... simultaneously detected photoelectrons to be resolved. This permits calibration of the number of ADC least counts per photoelectron, and thus interpretation of the detected light yield per fiber from cosmic rays (Fig. 6a) directly in terms of photoelectrons.

Gain: Fig. 7a displays the gain distribution for all 3072 channels of the CRT, where the gain for each channel is defined as the separation in ADC counts between the first photoelectron peak and the pedestal of the calibration spectrum for that channel. (Refer to Fig. 6b.) The gains are the same to within 10% for all channels. This gain distribution has been found to be stable over a period of months as Fig. 7b shows.

Gain Dispersion: Gain dispersion for a given channel is determined by comparing the measured width of the pedestal peak (assumed to consist of preamp/electronics noise only) and the width of the first photoelectron peak (which includes signal gain dispersion as well as the preamp/electronics component). We assume that the signal gain dispersion and preamp/electronics contributions combine in quadrature to form the width of the single photoelectron peak. Fig. 8a presents these measured widths for all 3072 channels, and as expected, the widths for the single photoelectron peaks are slightly larger than for the pedestals. The average signal gain dispersion for all channels is measured to be 14.7%. This quantity, like the gain itself, remains stable over long periods of time as Fig. 8b indicates.

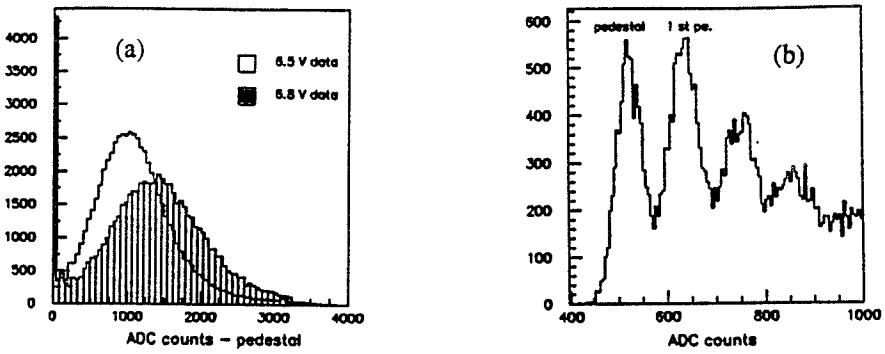

Figure 6. Signals from fiber/VLPC channels for: (a) cosmic ray triggers; (b) pulsed LED light injected into the end of a fiber.

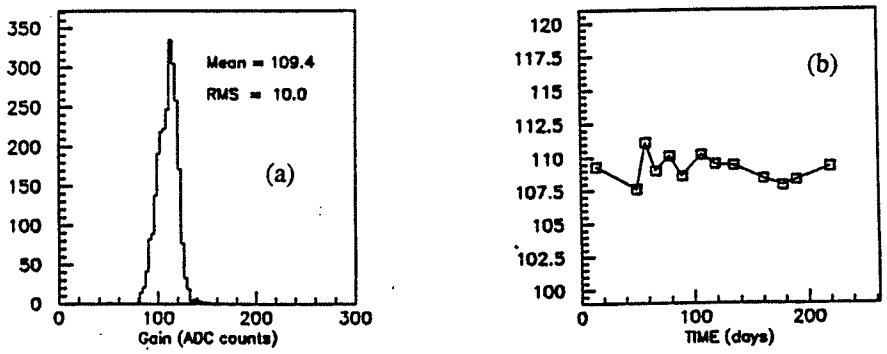

Figure 7. VLPC gain: (a) for all 3072 channels used in the Cosmic Ray Test facility, and (b) the dependence of the gain as function of time.

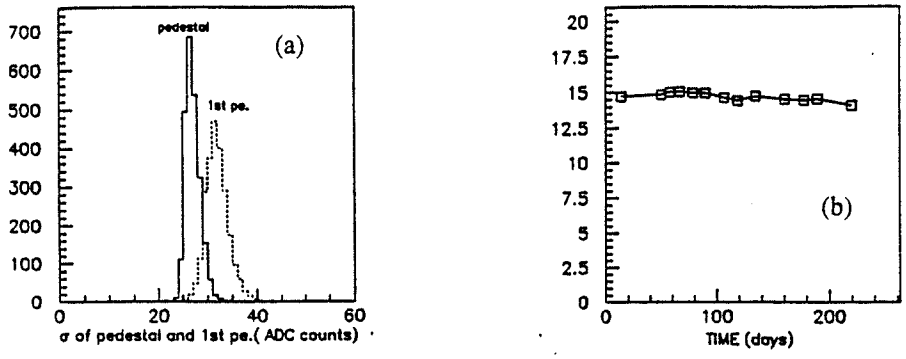

Figure 8. VLPC Gain Dispersion: (a) the meaured widths of pedestals and first photoelecton peaks for the 3072 channels of the Cosmic Ray Test facility, from which the averagé gain dispersion is determined; (b) the average gain dispersion as a function of time.

Photoelectron yield: After LED calibration of the individual fiber channels, and upon applying track reconstruction techniques to the cosmic ray triggered data, the photoelectron yield of single fibers may be obtained. To measure the average number of photoelectrons from fibers in a single fiber layer, tracks were reconstructed without the fiber doublet containing the singlet layer under study. The fit tracks were then extrapolated to that layer, and the pulse height of those fibers within 350 μm of the fitted trajectory were plotted. Fig. 6a displays the results for two VLPC bias voltages. The mean number of detected photoelectrons for a given bias is then obtained from Fig. 6a by dividing the average pulse height by the appropriate gain at that bias (109.4 ADC counts/pe at 6.5V; 139.5 ADC counts/pe at 6.8V). We obtain a mean of 9.6 detected photoelectrons at 6.5V bias and 10.0 detected photoelectrons at 6.8V bias. These results are consistent with earlier measurements [10], and affirm that high photoefficiency can be realized in a large scale system. In Fig. 9 are plotted the most probable number of photoelectrons for a given fiber layer in the CRT, which is 8.4 photoelectrons averaged over all layers. (Note the most probable photoelectron yield is ~ 0.5 pe less than the mean photoelectron yield.)

The photoelectron yield is stable over time for the 3072 channel CRT system. Figure 10 displays the time dependence of the mean ADC signal from the CRT data for several of the fiber layers. (Note the suppressed zero for the vertical scale.)

Noise: System noise is defined as the percentage of channels which are active (have signal) above some theshold in a given time window (a 100ns gate). Figure 11 compares the noise level measured in the CRT for signal thresholds in photoelectrons. The noise performance is excellent, with an 0.1% noise level corresponding to a conservative 1 pe threshold. These noise levels are for the HISTE-IV VLPCs which were the version of photosensors used in the CRT. This performance is expected to be improved still further (by a factor ≥ 10) with the new fabrication lot of HISTE-V VLPCs which have been recently delivered from Rockwell. The noise level is observed to be stable over a period of many months (Fig. 11b).

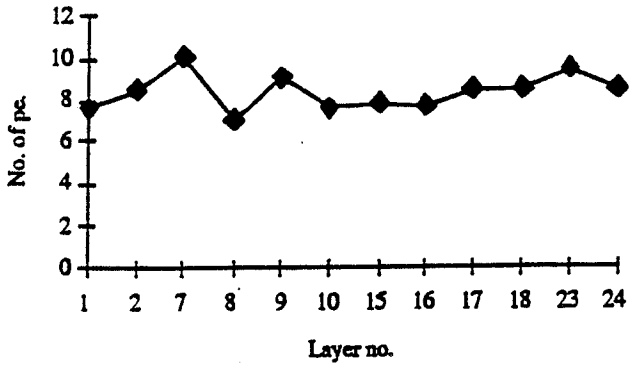

Figure 9. The most probable photoelectron yield for all fiber layers in the CRT system.

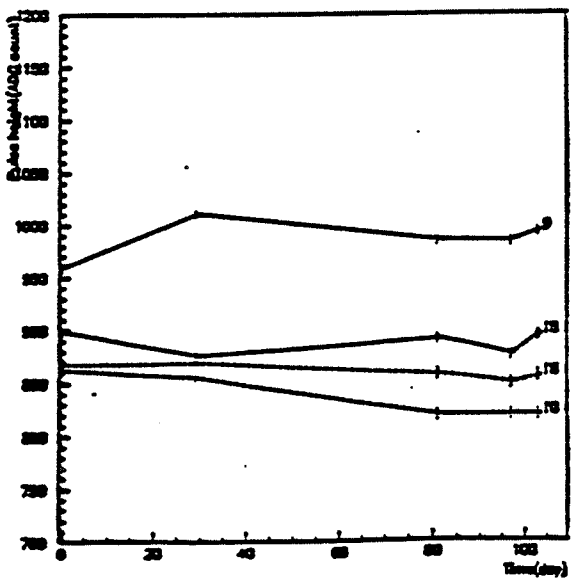

Figure 10. Measured mean photoelectron yield for several fiber doublet ribbons as a function of time. (Note the suppressed zero on the vertical scale.)

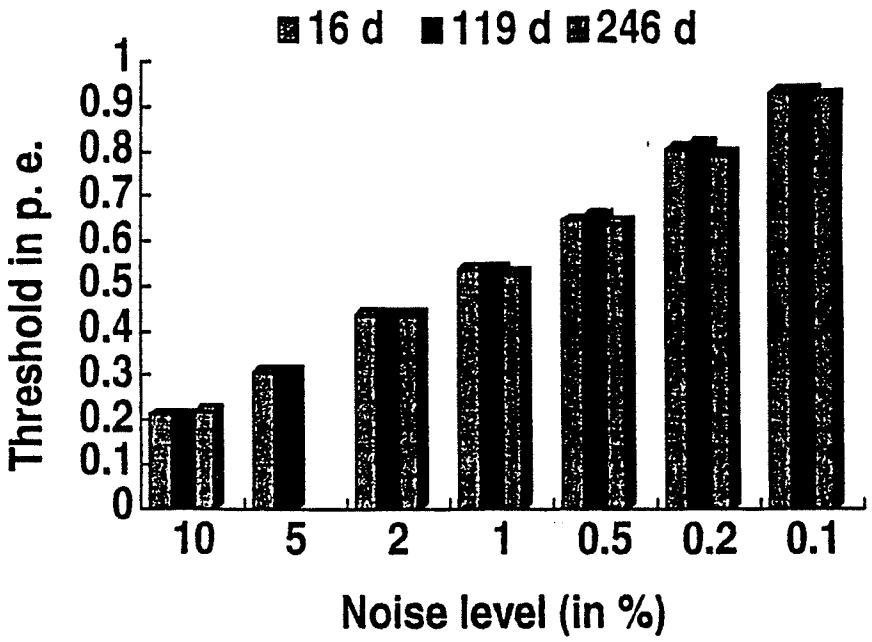

Figure 11. Noise rate stability of the scintillating fiber tracker prototype: (a) distribution of thresholds for a noise level of 0.1%; (b) thresholds in photoelectrons as a function of noise level.

Detector Efficiency: The efficiency of a fiber doublet has been determined by the following procedure. A cosmic ray track is reconstructed using all fiber layers except the particular doublet layer of interest. The track is projected to this doublet, and the four closest fibers to the trajectory are interrogated for pulseheight above threshold. Table 1 shows the noise level in percent and the fiber doublet efficiency after noise subtraction. Note that the 0.1% noise level corresponds to a threshold of 1 photoelectron. For reasonable threshold values, the fiber doublet efficiency exceeds 99%.

Noise level (in %)	Doublet efficiency after noise subraction
0.025	0.9960±0.0002
0.050	0.9953±0.0002
0.075	0.9944±0.0003
0.100	0.9933±0.0003
0.125	0.9925±0.0003

Table 1. Detection efficiency for fiber doublet layers for various noise levels.

Spatial Resolution: In Fig. 12 is displayed a typical residual distribution for a fiber doublet in the transverse (x) view, when that fiber doublet is not included in the track definition. The tracking resolution per doublet layer is found to be momentum dependent (because of multiple coulomb scattering) and is 136 μm for $p_{min} > 2.3$ GeV/c and 149 μm for $p_{min} > 0.8$ GeV/c.

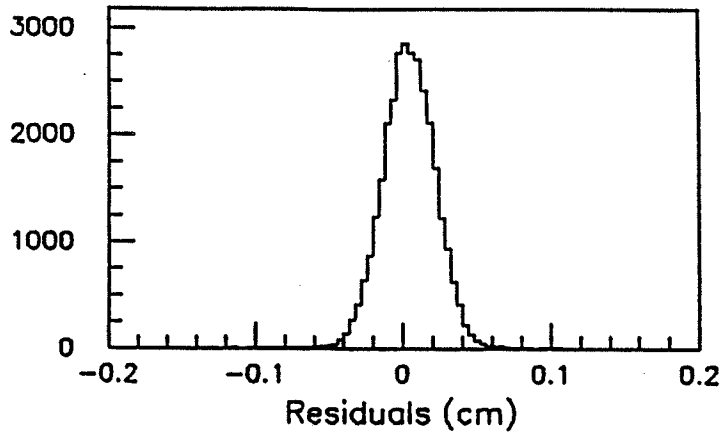

Figure 12. Spatial resolution for a fiber doublet.

Crosstalk: Optical crosstalk was studied using the calibration LEDs. A large LED pulse (30 pe equivalent) was injected into a given fiber, and the ADC spectra for that fiber and its neighbors were recorded. The neighbor spectra were examined for evidence of signal above pedestal. No signal was observed and we estimate the crosstalk to be less than 1%.

SUMMARY

The DØ Collaboration is building a central tracker consisting of 80,000 channels of scintillating fibers read out with visible light photon counters. A prototype system comrising 3,072 channels has been successfully operated and tested with cosmic rays for over 1 year. This cosmic ray test has demonstrated that in a large scale system of fibers and VLPCs, the detected photoelectron yield is high, the detection efficiency per fiber doublet exceeds 99%, and the operation is highly stable over a period of many months.

ACKNOWLEDGEMENTS

We thank the Fermilab Accelerator, Computing, and Research Divisions, and the support staffs at the collaborating institutions for the contributions to the success of this work. We also acknowledge the support of the U. S. Department of Energy, the U. S. National Science Foundation, the Commissariat à L'Energie Atomique in France, the Ministry for Atomic Energy and the Ministry of Science and Technology Policy in Russia, CNPq in Brazil, the Departments of Atomic Energy and Science and Education in India, Colciencias in Colombia, CONACyT in Mexico, the Ministry of Education, Research Foundation and KOSEF in Korea, and the A. P. Sloan Foundation.

REFERENCES

1. S. Abachi, et al, Nucl. Instr. and Methods A 338 (1994) 185.

2. S. Abachi, et al, Phys. Rev. Lett. 74 (1995) 2632; F. Abe, et al, Phys. Rev. Lett. 74 (1995) 2626.

3. "The D0 Upgrade", DØ Note 2542 (1995) and references cited therein.

4. "Conceptual Design Report for the DØ Upgrade", DØ Note 1733 and DØ Note 1933 (1993).

5. "Conceptual Design of a 2 Tesla Superconducting Solenoid for the Fermilab DØ Detector Upgrade", DØ Note 2167 (1994) and "DØ Solenoid Status - DØ Upgrade Director's Review", DØ Note 2429 (1995).

6. "DØ Silicon Tracker Technical Design Report", DØ Note 2169 (1994).

7. "Directors Review of the DØ Project", DØ Note 2159 (1994) and " Directors Review of the DØ Upgrade Project", DØ Notes 2427 and 2428 (1995). J. Warchol, SCIFI93 Workshop on Scintillating Fiber Detectors, edited by A.D.Bross, R.C.Ruchti, and M.R.Wayne, World Scientific (1995) 151.

8. "Physics Prospects with the DØ Upgrade", DØ Note 2671 (1995).

9. M. D. Petroff and M.G. Stapelbroek, IEEE Trans. Nucl. Sci. NS-36 (1) (1989) 158; and M. D. Petroff and M. Atac, IEEE Trans. Nucl. Sci. NS-36 (1) (1989) 163.

10. B. Baumbaugh, et al, Nucl. Instr. and Meth. A 345 (1994) 271.